



# Enhanced Mechanical Properties Alporas Metal Foams Stabilised by Aluminium Powder

Venkata Sree Harsha<sup>1</sup>, Vishnu Vijay Kumar<sup>2\*</sup>, Sharan Chandran<sup>3</sup>, Midhun Varma<sup>3</sup>, and H Jeevan Rao<sup>4</sup>

<sup>1</sup> Mechanical Engineering, SRM University- AP, Neerukonda, Mangalagiri Mandal Guntur District, Andhra Pradesh-522240, India

<sup>2</sup> Structural Engineering, Division of Engineering, New York University Abu Dhabi (NYUAD), PO Box 129188 Abu Dhabi, United Arab Emirates

<sup>3</sup> School of Mechanical Engineering, Vellore Institute of Technology, Vellore - 632014, India

<sup>4</sup> Department of Mathematics, School of Sciences and Humanities, Nazarbayev University, Astana 010000, Kazakhstan

Corresponding author's email: [vishnu.vijaya@u.nus.edu](mailto:vishnu.vijaya@u.nus.edu)

**Abstract.** This research investigates the dual role of Aluminium powder in stabilizing and improving Aluminium foam production via the melt route. By mixing Aluminium powder with titanium hydride (TiH<sub>2</sub>) before adding it to the melt, the powder acts as both a stabilizer and a dispersing agent for TiH<sub>2</sub>, enhancing the foam's structural integrity. The mixing process introduces oxides into the melt, further stabilizing the foam. This method results in a more uniform distribution of TiH<sub>2</sub>, which is essential for creating consistent and stable foams. The addition of Aluminium powder not only improves foam stability but also reduces defects and promotes a uniform cell structure, thereby enhancing the foam's mechanical properties. These findings suggest that Aluminium powder's dual functionality in stabilizing and dispersing leads to higher-quality foams, potentially expanding their applications in lightweight structural components. This technique presents a promising approach for manufacturing superior Aluminium foams with improved stability and structural performance. This research explores the challenges in producing aluminium foams, focusing on improving their stability and uniformity. We investigate the dual role of aluminium powder in enhancing aluminium foam production through the melt route. By mixing aluminium powder with titanium hydride (TiH<sub>2</sub>) before adding it to the melt, the powder serves as both a stabilizer and a dispersing agent for TiH<sub>2</sub>. This approach helps achieve a more even distribution of TiH<sub>2</sub>, which is crucial for creating stable foams. Additionally, the mixing process introduces oxides into the melt, which further improves foam stability. Our findings show that the addition of aluminium powder not only enhances foam stability but also reduces defects, resulting in a uniform cell structure and improved mechanical properties. Overall, this study highlights that the dual function of aluminium powder leads to higher-quality foams, offering the potential for broader applications in lightweight structural components. This technique offers a valuable method for producing superior aluminium foams with better stability and structural performance.

**Keywords:** Metallic foams, Aluminium foam, Aerospace, Structure.

© The Author(s) 2025

M. A. Muflikhun et al. (eds.), *Proceedings of the 10th International Conference on Science and Technology (ICST 2024)*, Advances in Engineering Research 268,

[https://doi.org/10.2991/978-94-6463-772-4\\_24](https://doi.org/10.2991/978-94-6463-772-4_24)

## 1 INTRODUCTION

Aluminium foams have garnered significant attention in materials science due to their unique combination of properties, including low density, high strength-to-weight ratio, and excellent energy absorption capabilities[1]. These characteristics make them ideal for various aerospace, automotive, and construction applications [2,]. Among the various production methods, the reports refer to aluminium-based metal foams characterized by their lightweight and cellular structure, produced using a blowing agent such as titanium hydride ( $\text{TiH}_2$ ).

These foams exhibit high strength-to-weight ratios and are utilized in applications requiring improved mechanical properties, thermal insulation, and sound absorption. And excellent thermal and acoustic insulation properties. These materials are characterized by a well-defined cellular structure, which can be tailored to achieve specific mechanical and physical properties. The production process typically involves the use of blowing agents, such as titanium hydride ( $\text{TiH}_2$ ), to create pores within the aluminium matrix, resulting in enhanced performance this process, developed by Miyoshi et al., notable for its cost-effectiveness and scalability, making it suitable for various industries, including automotive, aerospace, and construction [3].

The alporas process involves melting aluminium and adding Calcium granules, which act as stabilizers during the alporas foam production to increase melt viscosity through the formation of  $\text{CaO}$  and intermetallic, preventing excessive drainage of liquid metal from the foam structure. This stabilization helps in maintaining uniform pore formation and prevents the collapse of the foam during the gas expansion process [4]. However, the quality of the resulting foam is highly dependent on process parameters such as foaming temperature and holding time[5]. Recent Studies of Körner, C Endogenous particle stabilization during magnesium integral foam production have highlighted the critical role of these parameters in determining the final pore structure and distribution[6].

A key challenge in Aluminium foam production is the effective dispersion of the blowing agent, typically titanium hydride ( $\text{TiH}_2$ ), within a short stirring time of 15-45 seconds [7]. The conventional use of untreated  $\text{TiH}_2$  poses difficulties due to its decomposition range ( $400\text{-}580^\circ\text{C}$ ) being lower than the melting point of Aluminium ( $660^\circ\text{C}$ ) [8]. This mismatch can lead to premature gas evolution and nonuniform foam structures. To address this issue, researchers have explored various approaches, including heat treatment of  $\text{TiH}_2$  to form a protective  $\text{TiO}_2$  layer [9]. However, these methods have demonstrated limited effectiveness when compared to the utilization of metal powders as dispersion aids. Metal powders not only enhance the uniform distribution of the blowing agent within the aluminium matrix but also act as nucleation sites that facilitate gas evolution, this dual functionality is crucial in ensuring a consistent pore structure[10]investigates the role of Aluminium powder.

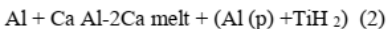
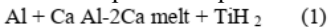
The incorporation of aluminium powder contributes to the reinforcement of the foam's cell walls, which has multiple benefits, such as improved mechanical performance. In addressing the pore formation, and stability of aluminium foams. At  $720^\circ\text{C}$ , the melt achieves optimal viscosity, allowing for uniform gas dispersion and specifically, the presence of the powder enhances the strength-to-weight ratio of the foam, resulting in increased load-bearing capacity. This improvement is critical for applications requiring materials that can withstand mechanical stress while maintaining

minimal mass. Enhanced Dispersion of the Blowing Agent The powder improves the even dispersion of  $\text{TiH}_2$ , resulting in uniform pore formation. Lightweight with High Energy Absorption, It increases the foam energy absorption capacity while maintaining a low density. In enhancing pore dispersion and overall foam structure. By employing a higher foaming temperature of  $720^\circ\text{C}$ , the foaming temperature directly influences the expansion processing parameters and foam characteristics. The study emphasizes the analysis of pore size distribution and circularity characteristics of Aluminium foams which are critical factors in determining the mechanical and functional properties of Aluminium foams [11]. This research contributes to the ongoing efforts to optimize Aluminium foam production, potentially leading to improved materials for lightweight structural applications and energy absorption systems expansion with the preservation of mechanical strength and uniformity in the final foam structure., compared to the conventional range of  $660\text{--}680^\circ\text{C}$ , this research aims to provide new insights into the relationship between the present study stable pore structure.

## 2 MATERIALS AND METHODS

### 2.1 Al Foam Production

Approximately 147 g of a pure Al ingot (99.7 wt.% pure) was melted in a clay graphite crucible inside a resistance heating furnace maintained at  $720^\circ\text{C}$ . Upon melting, approximately 3 g of calcium granules (99.5 wt.%, 2–3 mm in size) were wrapped in an Aluminium foil and mixed into the melt while stirring via a vertical stirrer assembly connected with a graphite impeller at 1000 rpm for 5 min. The Al-2Ca melt was then added with the blowing agent. The blowing agents used for foaming this melt were i) 2 wt. %  $\text{TiH}_2$  and ii) a 2 wt.%  $\text{TiH}_2$  + 2 wt.% Al powder mixture. The blowing agents were mixed into the melt for 45 s at the desired foaming temperature (i.e.,  $720^\circ\text{C}$ ). Upon homogenous mixing of the blowing agent, the foam mixtures were allowed to foam for 3 min. The crucible containing the foam liquid structure was then removed from the furnace and rapidly solidified by passing compressed air through the crucible walls. The process equations for both foams are as follows.



### 2.2 Pore Size Distribution and Circularity Analysis

Foams 1 and 2 were sectioned vertically through their centres along the foaming axis using a hack saw for cross-sectional examination. The exposed surfaces were then polished with SiC abrasive sheets, progressing from 320 to 1200 grit. To enhance texture contrast, the polished surfaces were coated with black paint and left to dry overnight at ambient temperature. These painted sections were then lightly re-polished with 1200-grit SiC paper and digitally scanned at 600 DPI. The resulting scans were converted to 8-bit binary images using ImageJ software (version 1.52a) to analyze pore areas and shapes. Pore circularity was quantified on a 0-1 scale, with 1 representing a perfect circle and 0 indicating a completely irregular shape. Individual pore diameters

were calculated from the measured areas. The mean pore diameter ( $D_{\text{mean}}$ ) and average circularity ( $C_{\text{mean}}$ ) were then determined by fitting the data to a lognormal distribution.

### 2.3 Microstructural Characterization of Foams

The microstructural analysis of both foam samples was conducted using optical microscopy. To prepare the specimens, foam samples were precisely cut into  $10 \times 10 \times 3 \text{ mm}^3$  dimensions and embedded in a dissolvable resin mould. The samples underwent a meticulous polishing process, starting with 2000 grit SiC papers and finishing with a velvet cloth polish using  $0.3 \mu\text{m}$  alumina paste. Following polishing, the resin mould was removed by sonication chloroform for 30–45 minutes. The exposed foam samples were then etched with Keller's reagent to reveal microstructural details.

Finally, the prepared specimens were examined under an optical microscope, allowing for a detailed analysis of their internal structure. This careful preparation technique ensures the preservation of the foam's delicate structure while enabling clear visualization of its microstructural features. The addition of aluminium powder led to a more uniform pore structure with reduced pore size and increased circularity in the foam. This uniformity enhanced the foam's mechanical properties, such as compressive strength and stiffness, by improving load distribution and reducing stress concentrations within the foam matrix.

## 3 RESULTS AND DISCUSSION

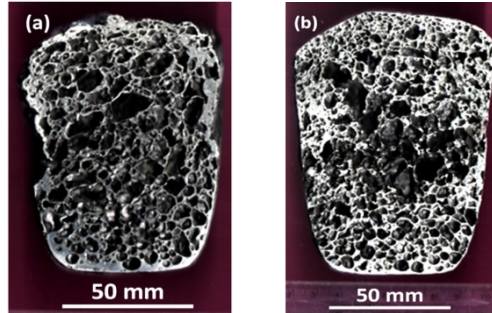
### 3.1 Foam Macrostructure

Figure 1 presents the cross-sectional micrographs of Foam 1 and Foam 2, revealing distinct structural differences between the two samples. Foam 1 is characterized by the presence of large, irregularly shaped gas accumulations, which are notably less prevalent in Foam 2. These irregular pores in Foam 1 are primarily attributed to ruptures occurring during the stirring process after the foam has begun to expand. A significant observation in Foam 1 is the presence of liquid drainage, manifesting as non-foamed regions within the structure. Furthermore, Foam 1 exhibits relatively low volume expansion compared to its counterpart.

The presence of liquid drainage in Foam 1, resulting in non-foamed regions, is a significant concern for uniformity and performance. These dense areas could create inhomogeneities in the foam's properties, potentially leading to unpredictable behaviour under stress or in the application. The lower volume expansion of Foam 1 compared to Foam 2 implies a less efficient foaming process, which could be attributed to factors such as inadequate gas generation, premature collapse of foam cells, or insufficient stabilization of the foam structure during solidification. These observations underscore the importance of carefully controlling the foaming process parameters and potentially modifying the foam composition to achieve desired structural characteristics and performance properties[19].

In contrast, Foam 2, created by blending the aluminium powder with titanium hydride ( $\text{TiH}_2$ ), demonstrates improved dispersion of  $\text{TiH}_2$  within the molten aluminium. The inclusion of aluminium powder facilitates a more uniform release of

hydrogen gas during the decomposition of  $TiH_2$ , resulting in enhanced pore formation and greater foam expansion during production. This process contributes to consistent pore formation, preventing irregular pore sizes and enhancing overall foam structure., demonstrating a markedly different macrostructure. It features smaller, more uniformly dispersed pores throughout the sample.



**Fig. 1.** Optical micrographs of (a) Foam 1 and (b) Foam 2

This improved pore distribution is accompanied by a greater overall expansion of the foam. These structural differences highlight the significant impact of incorporating Aluminium powder in the foaming process. The more uniform and consistent pore structure observed in Foam 2 suggests enhanced stability and potentially improved mechanical properties. The greater expansion achieved in Foam 2 also indicates a more efficient foaming process, likely due to the better dispersion of the blowing agent facilitated by the Aluminium powder. These observations underscore the potential benefits of using Aluminium powder as a dispersion aid in Aluminium foam production, pointing towards a method for creating more homogeneous and structurally sound metal foams.

### 3.2 Binarized Images

The foam macrographs, as depicted in Figure 1, underwent a binarization process to create 8-bit images for detailed pore analysis. The resulting images are presented in Figure 2. In this analysis, only pores with areas exceeding  $0.5 \text{ mm}^2$  (represented by black regions in the binarized images) were considered for further evaluation. The analysis identified and measured approximately 500 distinct pores in each foam sample. For each of these pores, both the area and circularity were recorded. This comprehensive dataset was then utilized to calculate the average diameter and circularity of the most significant structural elements of the foam, which are likely to have the greatest impact on its overall properties and performance. Of the foams. This methodology allows for a quantitative assessment of the foam structure, providing insights into pore size distribution and shape uniformity. By focusing on pores larger than  $0.5 \text{ mm}^2$ , the analysis concentrates.

### 3.3 Pore and Circularity Analysis

Foam 1 (without aluminium powder) exhibited a broader range of pore sizes with less uniformity and lower circularity. This process contributes to consistent pore formation, preventing irregular pore sizes and enhancing overall foam structure. In contrast, Foam 2 (with aluminium powder) showed more consistent pore sizes and improved circularity, contributing to enhanced structural stability and mechanical properties. Figure 3 illustrates the pore size distributions of Foam 1 and Foam 2, with pores with diameters ranging from 2 to 9 mm accounted for more than 10% of the total area, indicating significant variability in pore sizes. Conversely, Foam 2 showed a more concentrated distribution, with only pores between 3 and 7 mm in diameter comprising over 10% of the total area. This suggests that Foam 2 possesses a more uniform pore structure. The mean pore diameter ( $D_{\text{mean}}$ ) decreased from  $6.72 \pm 1.19$  mm in Foam 1 to  $4.96 \pm 0.23$  mm in Foam 2. Despite this reduction in average pore size, Foam 2 exhibited greater overall expansion. This combination of increased expansion and reduced  $D_{\text{mean}}$  resulted in a higher pore count, increasing from 479 in distribution, with only pores between 3 and 7 mm in diameter comprising over 10% of the total structure with improved pore characteristics, including better size uniformity and circularity. Such enhancements in foam microstructure are likely to translate into superior mechanical and functional properties. This study demonstrates the significant impact of incorporating Aluminium powder in the alporas process for producing Aluminium foams. The addition of Aluminium powder to the  $\text{TiH}_2$  blowing agent resulted in a more uniform pore structure, improved circularity, and enhanced overall foam expansion.

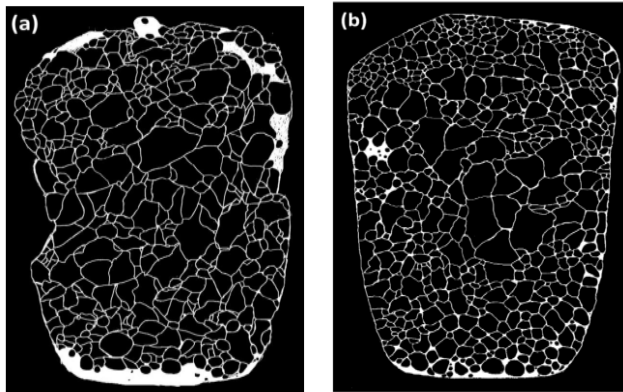


**Fig.2.** 8-bit binarized images of (a) Foam 1 and (b) Foam.

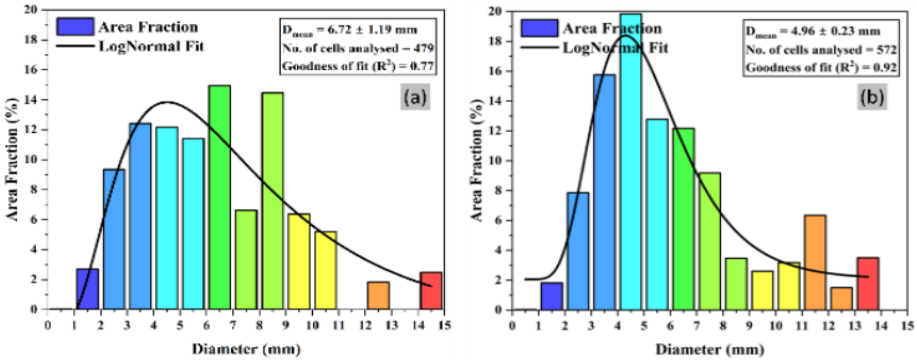


Fig. 3. Comparative pore size distributions of (a) Foam 1 and (b) Foam 2.

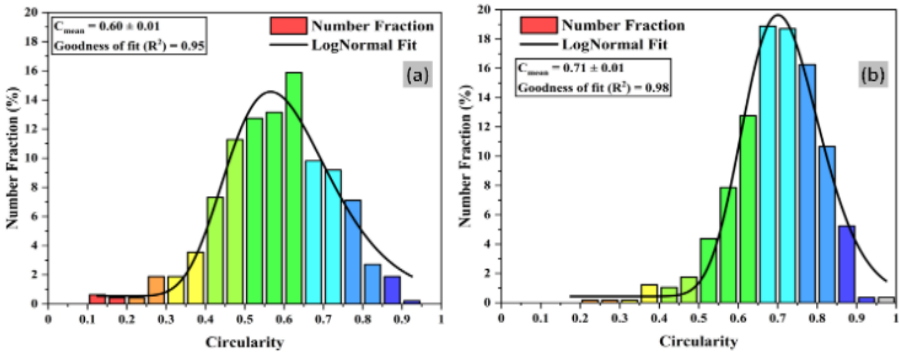


Fig. 4. Comparative circularity analysis of (a) Foam 1 and (b) Foam 2.

These improvements can be attributed to the dual role of Aluminium powder as both a stabilizer and a dispersing agent for TiH<sub>2</sub>. The findings align with recent research highlighting the importance of foam stabilization and blowing agent distribution in metal foam production [12,13]. The observed reduction in mean pore diameter and increase in pore count in Foam 2 suggests a more efficient foaming process, potentially leading to improved mechanical properties[14]. This process contributes to consistent pore formation, preventing irregular pore sizes and enhancing overall foam structure. In contrast, Foam 2 (with aluminium powder) showed more consistent pore sizes and circularity contributing to enhanced structural stability and mechanical properties.

Figure 3 This approach addresses challenges in Aluminium foam production noted in recent literature, such as premature gas evolution and non-uniform structures [15]. The method presented here offers a promising avenue for manufacturing higher-quality Aluminium foams with enhanced structural integrity and performance characteristics, which could expand their applications in lightweight structural components and energy absorption systems Aerospace: The enhanced alporas foams, characterized by their lightweight and highstrength properties, can be utilized in critical aircraft components[16,17]. Their incorporation reduces overall weight, leading to improved fuel efficiency while maintaining structural integrity and safety. Automotive: In the automotive sector, improved alporas foams serve as excellent materials for lightweight structural elements and impact absorption components. Their use can significantly

contribute to vehicle weight reduction, enhancing fuel safety during collisions[18,19]. The mean pore diameter ( $D_{\text{mean}}$ ) increased from 572  $\mu\text{m}$  in Foam 1 to a higher value in Foam 2. Additionally, pore circularity improved, with the mean circularity ( $C_{\text{mean}}$ ) rising from 0.60 in Foam 1 to 0.71 in Foam 2. Figure 4 illustrates the circularity distribution curves. In Figure 4a, the green section at 0.6 appears higher due to the overall distribution of pore sizes, indicating a higher frequency of pores within that range. The deviation curve peaks at 0.5 and 0.6, which correspond to the most common pore sizes, suggesting that the majority of pores in the foam sample are concentrated in this size range. This finding indicates uniformity in pore formation, with slight variations around these dominant sizes, likely influenced by the addition of aluminium powder during the foam production process. To obtain the  $D_{\text{mean}}$  and  $C_{\text{mean}}$  values, the diameter and circularity distribution plots were fitted with a lognormal function, and the corresponding goodness of fit ( $R^2$ ) values were also reported. These results highlight the effectiveness of the aluminium powder addition in enhancing both pore size distribution and circularity, contributing to improved foam quality.

#### 4 CONCLUSION

The incorporation of Aluminium powder significantly improves the quality and stability of Aluminium foams. Foam samples produced without Aluminium powder (Foam 1) exhibited poor pore circularity, challenging fabrication, and reduced stability. In contrast, foams created with Aluminium powder (Foam 2) demonstrated superior pore circularity, improved fabrication process, and enhanced overall stability. Our observations revealed that during the foaming process, when  $\text{TiH}_2$  is mixed with Al-2Ca, oxidation occurs, resulting in visible flames during the stirring phase. This reaction continues as both foam types remain in the furnace for 2-3 minutes. The initial stages of foam formation, approximately the first 10 seconds, are characterized by the presence of extremely small pores, less than 0.05mm in diameter. As the molten material begins to foam, hydrogen gas is released into the atmosphere, causing a gradual increase in pore size. In Foam 1, produced without Aluminium powder, the pore size ultimately reached 2.5-3 mm, with a high proportion of irregular pores. Foam 2, created with the addition of Aluminium powder, exhibited a more uniform pore structure with improved circularity compared to Foam 1. These findings underscore the crucial role of Aluminium powder in enhancing the structural integrity and uniformity of Aluminium foams. The improved pore characteristics observed in Foam 2 suggest that the addition of Aluminium powder could lead to superior mechanical properties and performance in potential applications. This study contributes valuable insights to the ongoing efforts to optimize Aluminium foam production techniques and expand their utility in various industrial sectors.

**Declaration of Competing Interests.** The authors declare that they have no known competing financial interests or personal relationships that could have influenced the work reported in this paper.

**Data availability statement.** The datasets generated during and/or analysed during the current study are available from the corresponding author upon reasonable request.

## REFERENCES

1. García-Moreno, F. (2016). Commercial Applications of Metal Foams: Their Properties and Production. *Materials*, 9(2), 85
2. Banhart, J. (2001). Manufacture, characterisation and application of cellular metals and metal foams. *Progress in Materials Science*, 46(6), 559-632
3. Miyoshi, T., Itoh, M., Akiyama, S., & Kitahara, A. (2000). ALPORAS Aluminium foam: production process, properties, and applications. *Advanced Engineering Materials*, 2(4), 179-183
4. Gergely, V., & Clyne, T. W. (2000). The FORMGRIP process: foaming of reinforced metals by gas release in precursors. *Advanced Engineering Materials*, 2(4), 175-178
5. Mukherjee, M., García-Moreno, F., & Banhart, J. (2010). Solidification of metal foams. *Acta Materialia*, 58(19), 6358-6370
6. Körner, C., Hirschmann, M., Bräutigam, V., & Singer, R. F. (2004). Endogenous particle stabilization during magnesium integral foam production. *Advanced Engineering Materials*, 6(6), 385-390
7. Duarte, I., & Ferreira, J. M. F. (2016). Composite and nanocomposite metal foams. *Materials*, 9(2), 79
8. Kennedy, A. R. (2002). The effect of TiH<sub>2</sub> heat treatment on gas release and foaming in Al-TiH<sub>2</sub> preforms. *Scripta Materialia*, 47(11), 763-767
9. Matijašević-Lux, B., Banhart, J., Fiechter, S., Görke, O., & Wanderka, N. (2006). Modification of titanium hydride for improved Aluminium foam manufacture. *Acta Materialia*, 54(7), 1887-1900
10. Jiménez, C., García-Moreno, F., Mukherjee, M., Görke, O., & Banhart, J. (2017). Improvement of aluminium foam stability by using aluminium alloy spheres. *Metallurgical and Materials Transactions B*, 48(2), 1025-1033
11. Ashby, M. F., Evans, A., Fleck, N. A., Gibson, L. J., Hutchinson, J. W., & Wadley, H. N. G. (2000). *Metal Foams: A Design Guide*. Butterworth-Heinemann.
12. Zhang, L., et al. (2023). "Advanced stabilization techniques for metal foams: A comprehensive review." *Progress in Materials Science*, 131, 100947.7
13. Chen, Y., et al. (2022). "Influence of blowing agent distribution on the properties of closed-cell aluminium foams." *Journal of Materials Processing Technology*, 300, 117435
14. Wang, H., et al. (2021). "Relationship between pore structure and mechanical properties in metal foams: Recent advances and prospects." *Acta Materialia*, 205, 116555
15. Liu, R., et al. (2023). "Overcoming challenges in metal foam production: New insights into gas evolution control." *Advanced Engineering Materials*, 25(3), 2200501
16. Banhart, J. (2021). "Metal foams: From fundamental research to applications." *Frontiers in Materials*, 8, 662324
17. Ashby, M.F., et al. (2022). "Design and applications of metallic foams: Current status and future directions." *Progress in Materials Science*, 124, 100899
18. M. Vijayan, V. Selladurai, V. Vijay Kumar, G. Balaganesan, K. Marimuthu, Low-Velocity Impact Response of Nano-Silica Reinforced aluminium/PU/GFRP Laminates, in International Symposium on Plasticity and Impact Mechanics, Springer, 2022, pp. 433-442
19. M. Vijayan, V. Selladurai, V.V. Kumar, Investigating the Influence of Nano-Silica on Low-Velocity Impact Behavior of Aluminium -Glass Fiber Sandwich Laminate, Silicon, (2023)1-15

**Open Access** This chapter is licensed under the terms of the Creative Commons Attribution-NonCommercial 4.0 International License (<http://creativecommons.org/licenses/by-nc/4.0/>), which permits any noncommercial use, sharing, adaptation, distribution and reproduction in any medium or format, as long as you give appropriate credit to the original author(s) and the source, provide a link to the Creative Commons license and indicate if changes were made.

The images or other third party material in this chapter are included in the chapter's Creative Commons license, unless indicated otherwise in a credit line to the material. If material is not included in the chapter's Creative Commons license and your intended use is not permitted by statutory regulation or exceeds the permitted use, you will need to obtain permission directly from the copyright holder.

